

DESIGN AND OPTIMISATION OF A STATIONARY CHEST TOMOSYNTHESIS SYSTEM WITH MULTIPLE FLAT PANEL FIELD EMITTER ARRAYS: MONTE CARLO SIMULATIONS AND COMPUTER AIDED DESIGNS*

T. G. Primidis^{1,2†}, C. P. Welsch¹, University of Liverpool, Liverpool L69 3BX, United Kingdom
V. Y. Soloviev, S. G. Wells, Adaptix Ltd, Oxford OX5 1PF, United Kingdom
¹also at The Cockcroft Institute, Warrington WA4 4AD, United Kingdom
²also at King's College London, London SE1 7EU, United Kingdom

Abstract

Digital tomosynthesis (DT) allows 3D imaging by using a $\sim 30^\circ$ range of projections instead of a full circle as in computed tomography (CT). Patient doses can be ~ 10 times lower than CT and similar to 2D radiography but diagnostic ability is significantly better than 2D radiography and can approach that of CT. Moreover, cold-cathode field emission technology allows the integration of 10s of X-ray sources into source arrays that are smaller and lighter than conventional X-ray tubes. The distributed source positions avoid the need for source movements and Adaptix Ltd has demonstrated stationary 3D imaging with this technology in dentistry, orthopaedics, veterinary medicine and non-destructive testing. In this work we present Monte Carlo simulations of an upgrade to the Adaptix technology to specifications suited for chest DT and we show computer aided designs for a system with various populations of these source arrays. We conclude that stationary arrays of cold-cathode X-ray sources could replace movable X-ray tubes for 3D imaging and different arrangements of many such arrays could be used to tailor the X-ray fields to different patient size and diagnostic objective.

INTRODUCTION

Adaptix Ltd have demonstrated veterinary and human cadaver extremity digital tomosynthesis (DT) with the devices shown in Fig. 1. Both are small and light enough to be carried by hand and have been operated safely in clinics and exhibitions globally. Demonstrated applications also include dental DT with human cadavers and non-destructive testing of electronics and composites [1].

Adaptix DT systems use a compact flat panel source (FPS) with a square array of emission positions. The FPS comprises electron field emitters etched on a silicon wafer in square arrays as shown in Fig. 2. In this design, all electron emitters turn on simultaneously with a 60-70 kV potential, but an electron beam steering module ensures only one electron beam at a time enters its respective collimator aperture to reach the X-ray target. The rest are absorbed in the bulk of the collimator. The FPS is coupled to a flat panel detector (FPD) to create the full DT system and both FPS and FPD remain stationary.

* Work funded by the Accelerators for Security, Healthcare and Environment Centre for Doctoral Training by the United Kingdom Research and Innovation Science and Technology Facilities Council; ID: ST/R002142/1.
† thomas.primidis@gmail.com

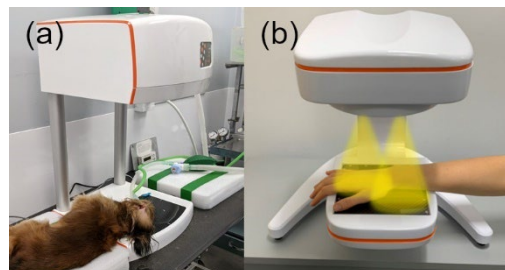


Figure 1: Adaptix (a) veterinary and (b) extremity DT systems. Reproduced with permission from Adaptix Ltd.

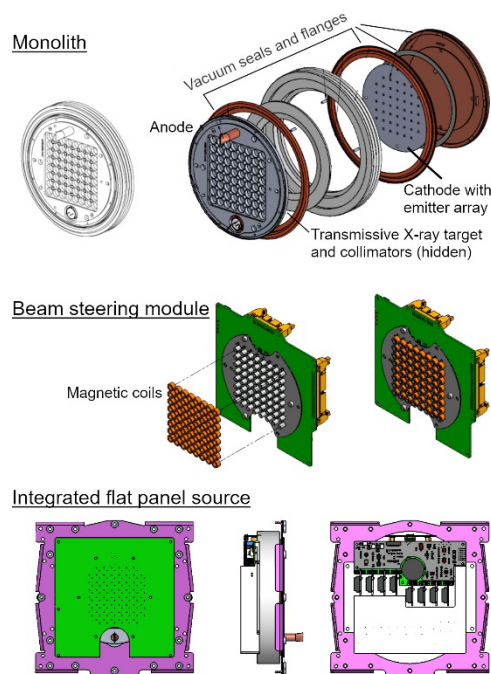


Figure 2: Schematics of the Adaptix FPS. Reproduced with permission from Adaptix Ltd.

DT uses a limited ($\sim 30^\circ$) angular range of projections instead of half-, full- or multi-circle scans used in computed tomography (CT) [2]. DT is a 3D X-ray imaging modality with a cost and dose comparable to 2D radiography but with image quality that can approach that of CT and literature suggests DT could be an alternative to both modalities on specific occasions [3-5].

The most requested X-ray exam is for the chest. In 2020-21 in England, 2D chest and 3D chest or abdomen X-ray imaging amounted to 80% (7.3 million) of all imaging

activity with tests suitable for diagnosing cancer [6]. But moving a sick patient to a radiology room can be risky. Also available mobile CT scanners use heavy X-ray tubes and batteries, making them nearly one-ton machines, difficult to store and transport [7-9]. Their size and price and the cost of CT scans can also be prohibitive for smaller clinics, in less developed areas or with smaller patient throughput. Moreover, CT dose can be prohibitive on follow-up or recurring scans.

But as mentioned before, DT is cheaper, gives ~10 times less dose than CT and could be a CT alternative on some occasions. Also, chest DT systems commonly operate at 120 kV, but 90 kV can produce similar image quality at a fixed effective dose (ED) [10] and even fixed emitted photon flux [11]. So, upgrading Adaptix' portable FPS DT systems to 90 kV could bring cheaper, lower dose chest 3D X-ray imaging to smaller clinics and more patients' bedside.

In this work, we present Monte Carlo (MC) simulations of this upgrade, and we introduce Iponi, our software for computer-aided designs (CAD) of multi-FPS DT systems necessary for covering the larger volume of the chest.

SINGLE FPS UPGRADE

Upgrading from 60-70 kV to 90 and 120 kV started with choosing an appropriate X-ray target thickness and accelerating voltage. FLUKA [12] MC simulations with a single monochromatic electron pencil beam of various energies incident perpendicularly on an infinitely wide, 20 μm thick X-ray target of undisclosed material revealed the combinations of accelerating voltage and target thickness with high photon yield as shown in Fig. 3. 3-6 μm were chosen as a reasonable target thickness range for 90 kV and 120 kV.

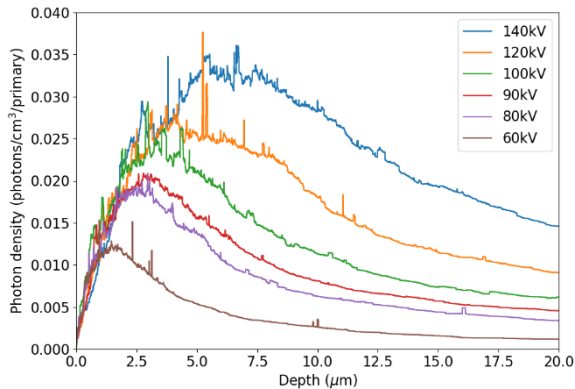


Figure 3: Simulated forward facing photon density versus X-ray target depth and electron accelerating potential.

With these specifications, the FLUKA simulation was repeated but now including the FPS filtration, namely the anode and the printed-circuit board from Fig. 2. The scored energy spectra shown in Fig. 4 reveal that 120 kV beams are 1.7-2.0 times as efficient as 90 kV beams which reach a plateau within this range of target thickness.

Figure 5 illustrates the attenuation of these spectra in aluminium (Al) simulated in FLUKA confirming that half-value layer is larger than the regulatory minima of 3.2 mm and 4.3 mm for 90 kV and 120 kV respectively [13,14]. 100 kV and 71 kV data are shown for completeness.

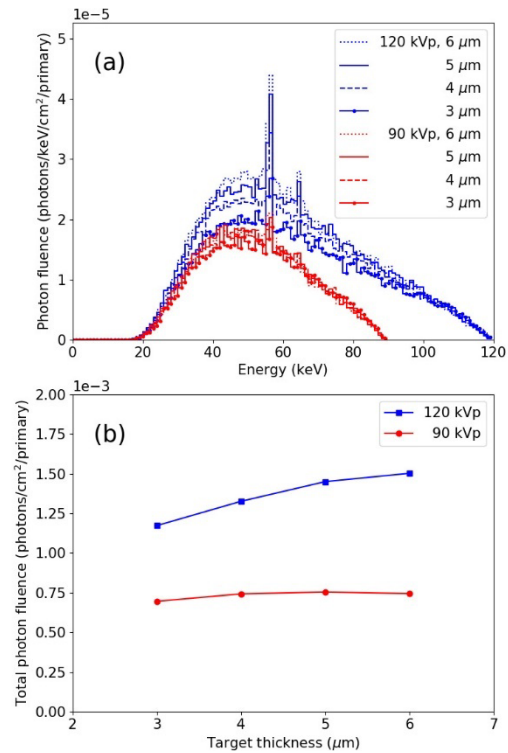


Figure 4: Simulated (a) energy spectra and (b) photon yield with different FPS designs. Adapted from [11] CC BY 3.0.

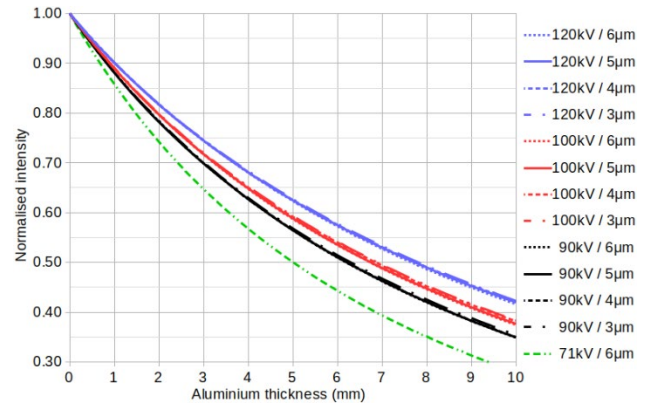


Figure 5: Single beam attenuation in Al of photon beams from different FPS designs.

Due to the higher photon yield and robustness of thicker targets, the spectra with 6 μm target were used to simulate end-to-end DT procedures with the two voltages. Shown in Fig. 6(a-b) is a 5x5, 2 cm pitch FPS array, the ICRP 145 adult male reference phantom [15] and a 43x43 cm² plane 80 cm away from the array, scoring photon fluence, acting as a FPD [16]. This geometry had an angular range of 8°.

The 25 sources were considered identical, so they were simulated in Geant4 [17] using the same model. X-ray beam shape and size were based on an existing Geant4 model of the 60 kV FPS [18] and energy spectra were those from Fig. 4a. We used Geant4 instead of FLUKA at this stage because it offered an easier way to load the phantom.

In Fig. 7, reconstructed 3D planes [19] with the two FPSs are similar within $\pm 10\%$; this agrees with literature on the similar image quality with 90 and 120 kV chest DT [10].

Content from this work may be used under the terms of the CC BY 4.0 licence (© 2022). Any distribution of this work must maintain attribution to the author(s), title of the work, publisher, and DOI

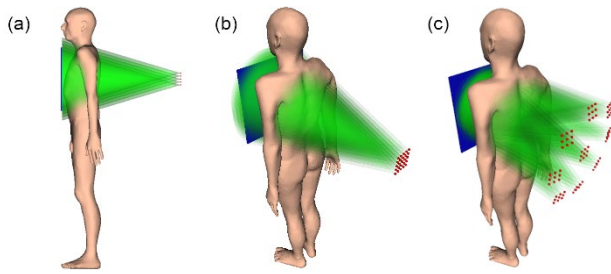


Figure 6: Irradiation geometry for chest DT using (a-b) a single flat panel source array and (c) multiple ones as designed by Ipioni. Reproduced from [11] CC BY 3.0.

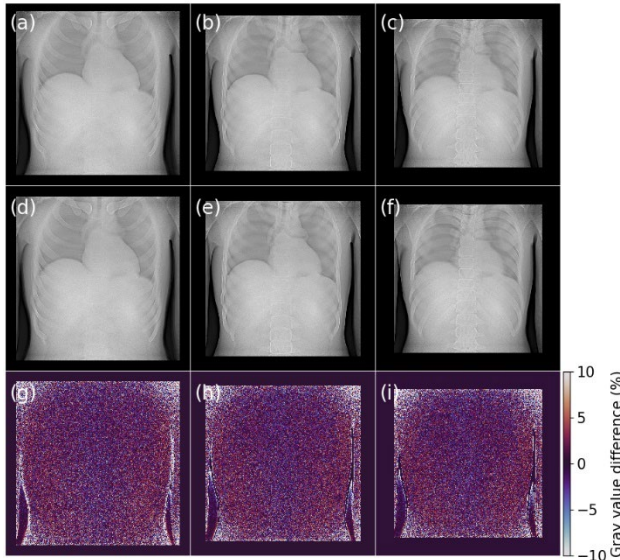


Figure 7: (a-c) Tomosynthesis slices at different depths using the 120 kV FPS, (d-f) same slices with the 90 kV FPS, (g-i) relative percentage difference between 120 kV and 90 kV. Reproduced from [11] CC BY 3.0.

ED was 0.113 mSv with 90 kV and 0.131 mSv with 120 kV [11] so there is clinical benefit in reducing the voltage. These values are also close to the 0.12 mSv of a clinically available chest DT system [20]. But this ED was calculated with 2.5 billion photons per X-ray source, initially chosen to reduce statistical error in dosimetry and images. With photon yield from Fig. 4b, 1 mm collimator aperture and 100 μ A per emitter suggested by Adaptix, each emitter needs 4.2 s and 2.1 s to produce that many photons with 90 kV and 120 kV respectively. Specifications are closer to 100 ms to reduce total scan time to <10 s so photon flux must be reduced to 1/42 for 90 kV and 1/21 for 120 kV. This increases the current projection image noise (\sim 3%) by a factor of $\sim\sqrt{42}=6.5$ for 90 kV and $\sim\sqrt{21}=4.6$ for 120 kV and 9 FPSs would lead to 9/42=21% and \sim 9/21=42% ED respectively. So, multi-FPS 3D DT can be delivered without excess ED and without excess image noise.

MULTI-FPS CAD

Ipioni is a Python CAD tool we developed for designing multi-FPS DT systems. It takes minimal input such as preferred number of FPSs and emitter array shape, FPD, patient and FPS dimensions, and any range of X-ray cone

angle, emitter pitch, source-to-image distance (SID) and panel angle in which to search for geometrically feasible designs. This feasibility includes clearance between FPSs and FPD and no overlaps between FPSs, patient and FPD since this is unphysical. Among the feasible designs, Ipioni identifies those that have optimum geometries so they can be studied with detailed MC simulations and experiments and eventually be built. Optimum geometries have minimum size and stray (outside the detector) radiation and maximum beam overlap, angular range and FPD coverage.

Ipioni designs DT systems with up to 9 FPSs, it exports data to be built with 3D CAD software as shown in Fig. 8 and Fig. 6c and plots X-ray beam profiles on the FPD and in the patient as shown in Fig. 9. Notice how all designs have no stray radiation and head and neck are spared in Fig. 6c. So, Ipioni provides a wealth of clinical and geometrical information about these complex devices, helping inform and accelerate their design and optimisation at an early stage, improving R&D efficiency and driving down costs.

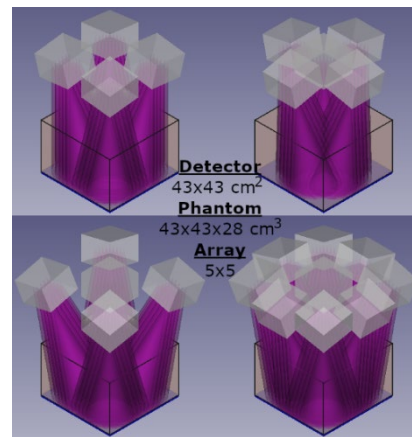


Figure 8: Multi-FPS DT systems designed by Ipioni and drawn in FreeCAD [21]. white boxes: FPSs, purple cones: X-ray beams, transparent box: phantom, blue box: FPD.

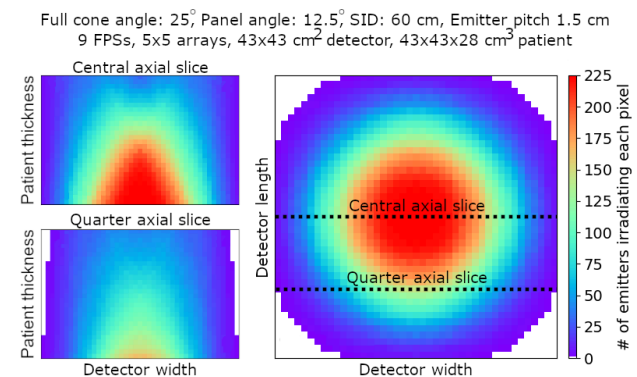


Figure 9: X-ray field plots by Ipioni.

CONCLUSION

FPSs allow 3D X-ray imaging of the human chest with similar image quality at 90 kV and 120 kV and lower ED at 90 kV. ED is low enough to allow multi-FPS systems which can better irradiate the patient and we have developed the necessary tools to automate the design of such multi-component systems quickly and efficiently.

REFERENCES

- [1] Adaptix Ltd, <https://www.adaptix.com>
- [2] C. Söderman *et al.*, “Detection of pulmonary nodule growth with chest tomosynthesis: a human observer study using simulated nodules”, *Acad. Radiol.*, vol. 26, p. 508–518, Apr. 2019. doi:10.1016/j.acra.2018.05.004
- [3] J. Vikgren *et al.*, “Comparison of chest tomosynthesis and chest radiography for detection of pulmonary nodules: human observer study of clinical cases”, *Radiology*, vol. 249, p. 1034–1041, Dec. 2008. doi:10.1148/radiol.2492080304
- [4] E. Quaia *et al.*, “Analysis of the impact of digital tomosynthesis on the radiological investigation of patients with suspected pulmonary lesions on chest radiography”, *Eur. Radiol.*, vol. 22, p. 1912–1922, Apr. 2012. doi:10.1007/s00330-012-2440-3
- [5] S.-H. S. Chou, G. A. Kieska, S. N. Pipavath, and G. P. Reddy, “Digital tomosynthesis of the chest: current and emerging applications”, *RadioGraphics*, vol. 34, p. 359–372, Mar. 2014. doi:10.1148/rg.342135057
- [6] National Health Service England and National Health Service Improvement, “Diagnostic Imaging Dataset Annual Statistical Release 2020-21”, Nov. 2021. <https://www.england.nhs.uk/statistics/statistical-work-areas/diagnostic-imaging-dataset/diagnostic-imaging-dataset-2020-21-data>
- [7] E. M. Nelson, S. M. Monazzam, K. D. Kim, J. A. Seibert, and E. O. Klineberg, “Intraoperative fluoroscopy, portable X-ray, and CT: patient and operating room personnel radiation exposure in spinal surgery”, *Spine J.*, vol. 14, p. 2985–2991, Dec. 2014. doi:10.1016/j.spinee.2014.06.003
- [8] Medtronic O-Arm™, <https://www.medtronic.com>
- [9] Siemens Healthineers ARCADIS Orbic®, <https://www.siemens-healthineers.com>
- [10] C. Söderman *et al.*, “Image quality dependency on system configuration and tube voltage in chest tomosynthesis-A visual grading study using an anthropomorphic chest phantom”, *Med. Phys.*, vol. 42, p. 1200–1212, Feb. 2015. doi:10.1118/1.4907963
- [11] T. G. Primidis, S. G. Wells, V. Y. Soloviev, and C. P. Welsch, “3D chest tomosynthesis using a stationary flat panel source array and a stationary detector: a Monte Carlo proof of concept”, *Biomed. Phys. Eng. Express*, vol. 8, p. 015006, Nov. 2021. doi:10.1088/2057-1976/ac3880
- [12] A. Fassò, A. Ferrari, J. Ranft, and P. R. Sala, “FLUKA: A multi-particle transport code (program version 2005)”, CERN, Geneva, Switzerland, Rep. CERN-2005-010; INFN-TC-2005-11; SLAC-R-773, Oct. 2005. doi:10.5170/CERN-2005-010
- [13] United States, Food and Drug Administration, “Performance standards for ionizing radiation emitting products”, 21 C.F.R. 1020, Government Publishing Office, Washington D.C., United States of America, Apr. 2021. <https://www.govinfo.gov/app/details/CFR-2021-title21-vol18/CFR-2021-title21-vol18-part1020>
- [14] European Commission, Directorate-General for Energy, “Criteria for acceptability of medical radiological equipment used in diagnostic radiology, nuclear medicine and radiotherapy”, Publications Office, Luxembourg, Luxembourg, MJ-XA-12-004-EN-C, Jan. 2013. doi:10.2768/22561
- [15] ICRP, 2020, “Adult mesh-type reference computational phantoms. ICRP Publication 145”, *Ann. ICRP* 49(3).
- [16] E. Skordis, C. P. Welsch, and V. Vlachoudis, “A Monte Carlo Approach to Imaging and Dose Simulations in Realistic Phantoms Using Compact X-Ray Source”, in *Proc. IPAC'17*, Copenhagen, Denmark, May 2017, pp. 4783–4786. doi:10.18429/JACoW-IPAC2017-THPVA137
- [17] S. Agostinelli *et al.*, “Geant4—a simulation toolkit”, *Nucl. Instrum. Meth. A*, vol. 506, p. 250–303, Jul. 2003. doi:10.1016/s0168-9002(03)01368-8
- [18] T. Primidis, V. Soloviev, and C. P. Welsch, “FLUKA and Geant4 Monte Carlo Simulations of a Desktop, Flat Panel Source Array for 3D Medical Imaging”, in *Proc. IPAC'21*, Campinas, Brazil, May 2021, pp. 2483–2486. doi:10.18429/JACoW-IPAC2021-TUPAB409
- [19] V. Y. Soloviev, K. L. Renforth, C. J. Dirckx, and S. G. Wells, “Meshless reconstruction technique for digital tomosynthesis”, *Phys. Med. Biol.*, vol. 65, p. 085010, Apr. 2020. doi:10.1088/1361-6560/ab7685
- [20] M. Bath, A. Svalkvist, A. von Wrangel, H. Rismyhr-Olsson, and A. Cederblad, “Effective dose to patients from chest examinations with tomosynthesis”, *Radiat. Prot. Dosim.*, vol. 139, p. 153–158, Mar. 2010. doi:10.1093/rpd/ncq092
- [21] FreeCAD (Version 0.19.2), <https://freecadweb.org>